

1 **RECENT RESULTS ON DIRECT CP**
2 **VIOLATION FROM NA48 EXPERIMENT AT**
3 **CERN**

4 A. BIZZETI^{1,2}

5 REPRESENTING THE NA48 COLLABORATION:

6 Cagliari, Cambridge, CERN, Dubna, Edinburgh, Ferrara, Firenze,
7 Mainz,

8 Orsay, Perugia, Pisa, Saclay, Siegen, Torino, Vienna, Warsaw

9 ¹*Dipartimento di Fisica dell'Università di Modena e Reggio Emilia, Modena, Italy*

10 ²*I.N.F.N., Sezione di Firenze, Sesto Fiorentino, Italy*

11
12 The direct CP violation parameter $\text{Re}(\varepsilon'/\varepsilon)$ has been measured from two-pion
13 decays of neutral kaons by the NA48 experiment at CERN SPS. The analysis
14 of a new data sample, collected in 2001 under different conditions compared
15 to earlier years (1997–99), provide the result: $\text{Re}(\varepsilon'/\varepsilon) = (13.7 \pm 3.1) \times 10^{-4}$.
16 Combining this result with that published from 1997–98-99 data, we obtain
17 an overall value $\text{Re}(\varepsilon'/\varepsilon) = (14.7 \pm 2.2) \times 10^{-4}$ from the NA48 experiment.

18 **1 Introduction**

19 CP violation was discovered in the neutral kaon system in 1964 [1] with
20 the first observation of the CP-forbidden decay $K_L \rightarrow \pi^+\pi^-$. If CP were
21 conserved, K_S and K_L particles would be pure CP eigenstates, decaying
22 only into $CP = +1$ and $CP = -1$ final states, respectively. The observa-
23 tion of $K_L \rightarrow 2\pi$ ($CP = +1$) decays provides a clear evidence of CP non
24 conservation.

25 The main component of CP violation is due to the mixing of the CP
26 eigenstates, called *indirect* CP violation and represented by the mixing
27 parameter ε . Another component, called *direct* CP violation and repre-
28 sented by the parameter ε' , may originate in the decay process through
29 the interference of amplitudes with different isospins.

30 In the Standard Model of electro-weak interactions, CP violation origi-
31 nates from an irreducible complex phase in the quark mixing matrix [2].

32 Current theoretical predictions of ε'/ε range from $\approx -10 \times 10^{-4}$ to \approx
 33 $+40 \times 10^{-4}$ [3].

The direct CP violation component is determined by measuring the double ratio R of partial decay widths, which is related to ε'/ε as follows¹:

$$R \equiv \frac{\Gamma(K_L \rightarrow \pi^0\pi^0)/\Gamma(K_S \rightarrow \pi^0\pi^0)}{\Gamma(K_L \rightarrow \pi^+\pi^-)/\Gamma(K_S \rightarrow \pi^+\pi^-)} \simeq 1 - 6 \operatorname{Re}(\varepsilon'/\varepsilon) \quad (1)$$

34 Results on direct CP violation were published by two experiments in
 35 1993: NA31 [4] measured $\operatorname{Re}(\varepsilon'/\varepsilon) = (23.0 \pm 6.5) \times 10^{-4}$, while E731 [5]
 36 measured $\operatorname{Re}(\varepsilon'/\varepsilon) = (7.4 \pm 5.9) \times 10^{-4}$.

37 More recently, NA48 published the measurement [6] $\operatorname{Re}(\varepsilon'/\varepsilon) = (15.3 \pm$
 38 $2.6) \times 10^{-4}$, obtained from the analysis of data collected in 1997 [7],
 39 1998 and 99, and KTeV presented a preliminary value [8] $\operatorname{Re}(\varepsilon'/\varepsilon) =$
 40 $(20.7 \pm 2.8) \times 10^{-4}$ from data accumulated in 1996 [9] and 1997. These
 41 results provide a convincing evidence of direct CP violation in the decay
 42 of neutral kaons.

43 We report here a measurement of $\operatorname{Re}(\varepsilon'/\varepsilon)$ performed by NA48 us-
 44 ing the 2001 data sample, recorded in different experimental conditions
 45 compared to earlier years. The main differences consist in the drift
 46 chambers, rebuilt after the implosion of the beam tube in november
 47 1999, and the SPS beam. Thanks to an extended SPS duty cycle, made
 48 possible after the closure of LEP, data were taken at a 30% lower instan-
 49 taneous beam intensity while keeping about the same per day statistics.

50 The 2001 data, equivalent to roughly half of the total 1998+99 statis-
 51 tics, have been used to check the insensitivity of the result to intensity-
 52 related effects and to complete the statistics for the final $\operatorname{Re}(\varepsilon'/\varepsilon)$ mea-
 53 surement.

54 2 The NA48 method

55 The double ratio R , from which $\operatorname{Re}(\varepsilon'/\varepsilon)$ is derived, is measured by count-
 56 ing the number of decays in each of the four decay modes. The experi-
 57 ment is designed to obtain cancellation of systematic effects contributing
 58 symmetrically to different components of the double ratio.

¹as the phase of ε' and that of $\varepsilon(\simeq -\pi/4)$ are very close, we get $\varepsilon'/\varepsilon \simeq \operatorname{Re}(\varepsilon'/\varepsilon)$.

59 The sensitivity of the measurement to accidental activity and to vari-
60 ations in beam intensity and detection efficiency is minimized by the si-
61 multaneous collection of the four decay modes in the same decay region.
62 Dead time conditions affecting any of the decay modes are recorded and
63 applied offline to all modes. In order to eliminate the effect of the small
64 and slow variations of the K_L and K_S beam intensities, K_S events are
65 further weighted by the K_L/K_S intensity ratio.

66 Two nearly-collinear neutral beams, converging to the center of the
67 electromagnetic calorimeter, provide K_L and K_S decays in the same fidu-
68 cial region with similar momentum spectra. In order to be insensitive
69 to residual differences in the beam momentum spectra, the analysis is
70 performed in bins of kaon energy.

71 The difference between K_L and K_S acceptances, due to different mean
72 decay lengths, is minimized by weighting the K_L decays as a function of
73 their proper lifetime, such that the K_L decay distribution becomes simi-
74 lar to the K_S one. The small remaining differences in beam divergences
75 and geometries are taken into account using a Monte Carlo simulation.

76 Decays from the K_S beam are identified by a coincidence between
77 the decay time and the registered times of the protons producing the K_S
78 beam.

79 Residual backgrounds which do not cancel in the double ratio are
80 minimized by identifying the $\pi^+\pi^-$ and $\pi^0\pi^0$ decays with high-resolution
81 detectors.

82 A detailed description of the NA48 experimental apparatus and of
83 the analysis of 1998–99 data can be found in [6].

84 **3 Beams, detectors and triggers**

85 The NA48 K_L and K_S simultaneous beams [10] are produced in two dif-
86 ferent targets by 400 GeV/c protons from the same SPS beam, having a
87 cycle time of 16.8 s and a spill length of 5.2 s.² The ratio of their inten-
88 sities is stable within 10%. The K_L beam intensity in 2001, measured
89 from the number of selected K_L decays as a function of time within the
90 extraction, is shown in Fig. 1 together with the intensity measured on
91 1999 data.

²The beam momentum was 450 GeV/c, the cycle time 14.4 s and the spill length 2.4 s in the 1997, 1998 and 1999 runs.

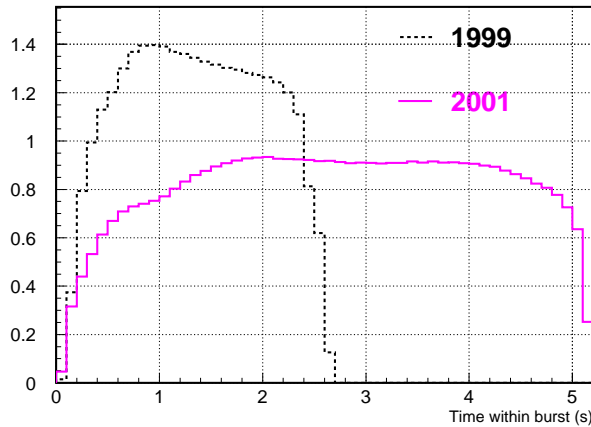


Figure 1: Rate of selected K_L events along the proton burst (in 0.1 s bins), proportional to the K_L beam intensity, in 2001 and 1999 data taking periods.

92 An array of scintillators [11] (Tagger) is used to record the time of
 93 protons producing the K_S beam. An anti-counter [12] (AKS), formed by
 94 a photon converter and three scintillation counters is located on the K_S
 95 beam at the beginning of the decay region.

96 Charged particles are measured by a magnetic spectrometer [13],
 97 consisting of a dipole magnet giving a momentum kick of 265 MeV/c
 98 and four drift chambers, with a momentum resolution $\sigma_p/p = 0.48\% \oplus$
 99 $0.009\% \times p/(1 \text{ GeV}/c)$. A scintillator hodoscope composed of two planes of
 100 orthogonal strips is located after the spectrometer to provide a precise
 101 time measurement for charged particles. The signals from hodoscope
 102 strips are combined in four quadrants by a fast logic electronics for the
 103 first level of the $\pi^+\pi^-$ trigger.

104 The energy, impact point and arrival time of photons from $\pi^0\pi^0$ events
 105 are measured by a quasi-homogeneous liquid krypton (LKr) electromag-
 106 netic calorimeter [14] with a projective tower read-out. The energy reso-
 107 lution is $\sigma_E/E = 3.2\%/\sqrt{E} \oplus 9\%/E \oplus 0.42\%$ (E in GeV), the spatial reso-
 108 lution better than 1 mm above 25 GeV.

109 An iron-scintillator hadron calorimeter is located downstream of the
 110 electromagnetic calorimeter, followed by a muon counter made of three
 111 planes of scintillator separated by 80 cm thick iron walls.

112 The beam intensities are measured by two beam counters, one of

113 which (K_L monitor) located at the end of the beam line, the other (K_S
114 monitor) near the target originating the K_S beam. Additional high-rate
115 beam monitors have been installed before the 2001 run, the one for the
116 K_S beam located near the Tagger, allowing to measure beam structures
117 down to ≈ 200 ns.

118 About 4×10^5 particles per second reach the NA48 detectors. The
119 trigger system is designed to reduce this rate to less than 10 kHz, with
120 minimal loss from dead time and inefficiencies. The small inefficiencies
121 of the main ($\pi^+\pi^-$ and $\pi^0\pi^0$) triggers are directly measured using data
122 selected by redundant low-bias triggers. Other triggers, initiated by the
123 beam monitors, are used to record the accidental activity with rates pro-
124 portional to the K_L and K_S beam intensities.

125 The trigger for $\pi^0\pi^0$ decays [15] makes use of the vertical and horizon-
126 tal projections of the LKr calorimeter to reconstruct the total deposited
127 energy, the longitudinal decay position and the extrapolated kaon im-
128 pact point.

129 A two-level trigger system is used for the $\pi^+\pi^-$ events. The first
130 level reduces the rate to about 100 kHz using a coincidence of three
131 fast signals: opposite quadrant coincidence in the scintillator hodoscope,
132 hit multiplicity in the first drift chamber and total calorimetric energy
133 above a threshold of 35 GeV. At the second level [16], a farm of asyn-
134 chronous microprocessors performs a fast event reconstruction using
135 data from the drift chambers and selects events compatible with a $K \rightarrow$
136 $\pi^+\pi^-$ decay.

137 4 Data analysis

138 4.1 Event selection

139 The $K \rightarrow \pi^0\pi^0$ events are selected requiring four in-time photons de-
140 tected by the electromagnetic calorimeter. From their measured ener-
141 gies and impact points, the decay vertex position along the beam axis is
142 reconstructed imposing that the four-photon invariant mass corresponds
143 to the kaon mass. The invariant masses of the two photon pairs are then
144 computed (with resolution better than 1 MeV/ c^2) and a χ^2 variable for the
145 $\pi^0\pi^0$ hypothesis is calculated. A cut is applied on this variable in order
146 to reject the residual background from $K_L \rightarrow 3\pi^0$ events.

147 The $K \rightarrow \pi^+\pi^-$ events are selected using informations from the spec-
 148 trometer. Both the longitudinal and transverse positions of the decay
 149 vertex can be determined, with resolutions of about 50 cm and 0.2 cm,
 150 respectively. Since the beams are vertically separated by about 6 cm in
 151 the decay region, a clean identification of the K_S and K_L decays is there-
 152 fore possible using the reconstructed vertex position. A cut is applied on
 153 the asymmetry $\mathcal{A} = |p_1 - p_2|/(p_1 + p_2)$ between the two tracks momenta
 154 in order to remove asymmetric decays in which one of the tracks could
 155 be close to the beam pipe, where the Monte Carlo modelling is more dif-
 156 ficult. Backgrounds from $\Lambda \rightarrow p\pi^-$ and $\bar{\Lambda} \rightarrow \bar{p}\pi^+$ are almost completely
 157 eliminated by this cut.

158 Background from semileptonic K_L decays is strongly suppressed by
 159 rejecting events with a track consistent with being either an electron or
 160 a muon. Electrons are rejected by requiring the ratio E/p of the energy
 161 deposited by the track in the LKr calorimeter over the track momentum
 162 to be less than 0.8. Muons are rejected by requiring no in-time hits in
 163 the muon counters near the track impact point. A further background
 164 suppression is achieved by applying kinematic cuts on the two-pion in-
 165 variant mass $m_{\pi\pi}$ and on the kaon transverse momentum p'_T .

166 4.2 K_S tagging

167 A decay is labeled K_S if a coincidence is found (within a ± 2 ns time inter-
 168 val) between the event time and a proton time measured by the Tagger;
 169 otherwise the decay is labeled K_L .

170 The time distributions for kaon decays to $\pi^+\pi^-$ final states, identified
 171 as K_S or K_L by their vertex position, is shown in Fig. 2. As tagging is the
 172 only available way to distinguish K_S from K_L in $\pi^0\pi^0$ decays, this method
 173 is used for both $\pi^0\pi^0$ and $\pi^+\pi^-$ modes. The double ratio is therefore
 174 sensitive only to differences in misidentification probabilities between
 175 the two decay modes and not to their absolute values, so that systematic
 176 effects are mostly symmetric.

177 The probability α_{SL} that, due to coincidence inefficiencies, a K_S decay
 178 is identified as a K_L , is called *tagging inefficiency*. In the $\pi^+\pi^-$ mode
 179 it is directly measured (using the vertical vertex position) to be $\alpha_{SL}^{+-} =$
 180 $(1.12 \pm 0.03) \times 10^{-4}$ and is found to be dominated by the Tagger inefficiency.

181 The difference between the tagging inefficiencies in $\pi^+\pi^-$ and $\pi^0\pi^0$
 182 decays is estimated by comparing the time measurements obtained from

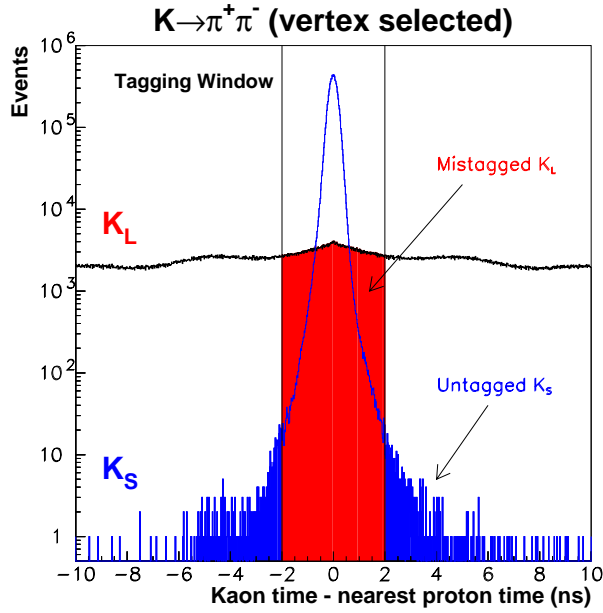


Figure 2: Time coincidence with nearest proton in the Tagger, for K_S and K_L decays to $\pi^+\pi^-$ identified by their reconstructed vertex.

183 the LKr calorimeter and from the scintillator hodoscope in $2\pi^0$ and $3\pi^0$
 184 events where one of the photons converts into an electron-positron pair.

185 The $\pi^0\pi^0$ and $\pi^+\pi^-$ tagging inefficiencies agree within an uncertainty
 186 of $\pm 0.5 \times 10^{-4}$, corresponding to an uncertainty on R of $\pm 3 \times 10^{-4}$.

187 The probability α_{LS} that, due to an accidental coincidence between
 188 the event and a proton, a K_L decay is identified as a K_S , is called *ac-*
 189 *cidental tagging*. It is measured in the $\pi^+\pi^-$ mode and results to be³
 190 $\alpha_{LS}^{+-} = (8.115 \pm 0.010) \times 10^{-2}$.

191 The difference $\Delta\alpha_{LS}$ between the α_{LS} values in $\pi^0\pi^0$ and $\pi^+\pi^-$ decays
 192 is determined by measuring the probability to find a proton within time
 193 windows 4 ns wide, located before or after the event time in K_L events.

194 The resulting value of $\Delta\alpha_{LS} \equiv \alpha_{LS}^{00} - \alpha_{LS}^{+-} = (+3.4 \pm 1.4) \times 10^{-4}$ corre-

³It was $(10.649 \pm 0.008) \times 10^{-2}$ in the 1998–99 data sample.

195 sponds to a correction on R of $(+6.9 \pm 2.8) \times 10^{-4}$.

196 **4.3 Definition of the decay region**

197 Events are counted within the following fiducial ranges in kaon energy
198 E_K and proper time τ : $70 \text{ GeV} < E_K < 170 \text{ GeV}$; $0 < \tau < 3.5\tau_S$, where
199 $\tau = 0$ corresponds to the position of the AKS counter and τ_S is the K_S life-
200 time. For K_L decays, the proper time cut is applied on the reconstructed
201 τ , while for K_S the lower cut is applied using the AKS to veto decays oc-
202 ccurring upstream. The nominal $\tau = 0$ position defined by the AKS differ
203 by $21.0 \pm 0.5 \text{ mm}$ between $\pi^+\pi^-$ and $\pi^0\pi^0$ decays, resulting in a correction
204 on R of $(+1.2 \pm 0.3) \times 10^{-4}$.

205 $K_S \rightarrow \pi\pi$ decays can be produced in both beams by scattering of beam
206 particles in the collimators and, in the K_S case, in the AKS counter. To
207 reduce this contamination, the extrapolated kaon impact point on the
208 LKr calorimeter is required to be within 10 cm of the intersecting beam
209 axes.

210 **5 Calculation of R and systematic uncertainties**

211 The calculation of R is performed dividing the data into 20 bins in kaon
212 energy, each bin 5 GeV wide. The numbers of K_S and K_L candidates,
213 corrected for the mistagging probabilities, are shown in Table 1.

Table 1

Number of events (corrected for mistagging).		
	$\rightarrow \pi^0\pi^0$	$\rightarrow \pi^+\pi^-$
K_L	1.546×10^6	7.136×10^6
K_S	2.159×10^6	9.605×10^6

214 Corrections for trigger inefficiencies, background subtraction, and
215 residual acceptance differences between K_S and K_L are applied sepa-
216 rately in each energy bin before computing the average of R .

217 Corrections and systematic uncertainties from mistagging and AKS
218 have already been discussed in the previous Section.

219 5.1 Trigger efficiencies

220 Events triggered by a scintillating fiber detector located inside the LKr
221 calorimeter have been used to measure the $\pi^0\pi^0$ trigger efficiency, which
222 results to be $(99.901 \pm 0.015)\%$. As this efficiency is $K_S - K_L$ symmetric,
223 no correction to the double ratio needs to be applied.

224 $(98.697 \pm 0.017)\%$. The difference in this efficiency between K_S and
225 K_L decays is computed in each energy bin, and the overall correction to
226 the double ratio results to be $(+5.2 \pm 3.6) \times 10^{-4}$, where the uncertainty
227 is given by the statistics of the control samples used to measure the
228 efficiency.

229 5.2 Backgrounds

230 The only background affecting the $K_L \rightarrow \pi^0\pi^0$ data comes from $K_L \rightarrow 3\pi^0$
231 decays, while the K_S mode is background free. The $K_L \rightarrow 3\pi^0$ back-
232 ground, uniformly distributed in the χ^2 variable, is estimated using a
233 control region in the χ^2 distribution. The excess of K_L candidates in this
234 region over a Monte Carlo expectation for $\pi^0\pi^0$ decays is used to extrap-
235 olate the background in the signal region. Background subtraction is
236 performed in kaon energy bins; the overall correction to the double ratio
237 is $(-5.6 \pm 2.0) \times 10^{-4}$.

238 Two control regions in the $m_{\pi\pi} - p_T'^2$ plane are used to estimate the
239 residual K_{e3} and $K_{\mu3}$ backgrounds in the $K_L \rightarrow \pi^+\pi^-$ sample. The back-
240 ground distributions in these control regions are modelled by a K_{e3} sam-
241 ple, selected with $(E/p)_e > 0.95$, and by a $K_{\mu3}$ sample, obtained by re-
242 versing the muon veto requirement. The tails in the $K_L \rightarrow \pi^+\pi^-$ dis-
243 tribution are estimated from the K_S sample. The result is then extrap-
244 olated to the signal region, obtaining for the K_{e3} and $K_{\mu3}$ background
245 fractions the values 10.5×10^{-4} and 3.0×10^{-4} , respectively. These back-
246 grounds are subtracted in kaon energy bins, resulting in a correction to
247 R of $(+14.2 \pm 3.0) \times 10^{-4}$.

248 In the K_S beam, the cut on the extrapolated kaon impact point is
249 stronger than the $p_T'^2$ cut applied to the $\pi^+\pi^-$ events. As a consequence,
250 beam scattering events are removed in the same way from both $\pi^0\pi^0$ and
251 $\pi^+\pi^-$ samples. On the contrary, in the K_L beam the $p_T'^2$ cut applied only
252 to the $\pi^+\pi^-$ events is stronger, therefore a small residual contribution
253 from scattering is left only in the $\pi^0\pi^0$ sample. The correction for this
254 effect is determined using $K_L \rightarrow \pi^+\pi^-$ candidates with an inverted $p_T'^2$

255 cut and applied in kaon energy bins. The resulting overall correction to
256 the double ratio is $(-8.8 \pm 2.0) \times 10^{-4}$.

257 **5.3 Acceptance**

258 The difference between K_S and K_L acceptances is minimized (in both
259 decay modes) by weighting K_L events according to their proper decay
260 time.

261 The small residual difference, due to the different beam sizes and
262 directions, is computed using a large-statistics Monte Carlo simulation
263 (4×10^8 generated kaon decays per mode). The resulting correction to R
264 is $(+21.9 \pm 3.5_{\text{MCstat}} \pm 4.0_{\text{syst}}) \times 10^{-4}$.

265 **5.4 Event reconstruction**

266 Kaon energy, decay vertex and proper time in the $\pi^0\pi^0$ events are de-
267 termined using the photon energies and positions measured with the
268 LKr calorimeter. The absolute energy scale is fixed using $K_S \rightarrow \pi^0\pi^0$
269 events and the known position of the AKL counter. Special runs (so-
270 called η runs) with a π^- beam striking two thin targets located near the
271 beginning and the end of the fiducial decay region have been used to
272 cross-check the energy scale with two-photon decays of prompt π^0 and η
273 mesons.

274 Linearity and spatial uniformity in the energy response are studied
275 using K_{e3} decays, where the electron energy measured with the calorime-
276 ter can be compared to the momentum measured with the spectrometer,
277 and using data from η runs. Position measurements with the calorime-
278 ter are also checked using K_{e3} data.

279 The total systematic error on the double ratio from the measurement
280 of the photon energies and positions results to be $\pm 5.3 \times 10^{-4}$.

281 The uncertainty on R from the reconstruction of $\pi^+\pi^-$ decays, due to
282 uncertainties in the detector geometry, is estimated to be $\pm 2.8 \times 10^{-4}$.

283 **5.5 Intensity effects**

284 The accidental activity in NA48 detectors is mainly produced by kaon
285 decays in the high-intensity K_L beam. The overlap of extra particles
286 with a good event may result in the loss of the event at the trigger or

287 data analysis level. The effect on R is minimized by the simultaneous
288 collection of the four decay modes and by the fact that K_S and weighted
289 K_L decays illuminate the detector in a similar way.

290 The possible residual effect can be separated into two components.
291 The first one (intensity difference) is caused by intensity variations be-
292 tween the two beams coupled to different, intensity-dependent, event
293 losses in the $\pi^+\pi^-$ and $\pi^0\pi^0$ modes. The other one (illumination differ-
294 ence) originates from a residual difference in the illumination between
295 K_S and K_L decays coupled to a dependence of the event loss probability
296 on the impact points of the kaon decay products.

297 Assuming a linear dependence of the event loss probability on the K_L
298 beam intensity, the intensity difference effect is given by $\Delta R = \Delta\lambda \times$
299 $\Delta I/I$, where $\Delta\lambda$ is the difference between the mean losses in $\pi^+\pi^-$ and
300 $\pi^0\pi^0$ modes and $\Delta I/I$ is the relative difference between the average K_L
301 beam intensity as seen by K_L and K_S events. The latter is measured in
302 different ways: from detector activity within the readout time window
303 before the event, from K_L beam monitor counts integrated over a 200 ns
304 time window and from the correlation between K_S and K_L beams, com-
305 puted using beam monitor counts taken at regular times during beam
306 extraction. All methods agree with a zero result within a $\pm 1\%$ uncer-
307 tainty.

308 $\Delta\lambda$ is estimated by overlaying data and Monte Carlo events with
309 events taken with the beam monitor trigger, and is found to be $(1.0 \pm$
310 $0.5) \times 10^{-2}$, with a linear dependence on the beam intensity, as expected.
311 The uncertainty on R from the intensity difference effects results to be
312 $\pm 1.1 \times 10^{-4}$, significantly better than in 1998–99 data due to the lower
313 beam intensity and improved beam monitors.

314 The illumination difference effect is also estimated using the overlay
315 technique. The corresponding uncertainty on the double ratio is evalu-
316 ated to be $\pm 3.0 \times 10^{-4}$.

317 The effects of additional “in-time” detector activity, generated by the
318 same collision in the K_S target producing the K_S event, are not taken
319 into account by the methods described above. These effects have been
320 studied mainly by searching, in $\pi^0\pi^0$ events from pure K_S beam runs, for
321 additional energy clusters in the LKr calorimeter. The effect on R is less
322 than 1×10^{-4} .

323 **6 Results**

324 A summary of the corrections applied to R and of the systematic un-
 325 certainties on the double ratio is shown in table 2, together with the
 326 corresponding values obtained in the analysis of 1998–99 data [6].

Table 2

Corrections and systematic uncertainties on R , in 10^{-4} units			
	2001	1998–99	
$\pi^+\pi^-$ trigger inefficiency	5.2 ± 3.6	-3.6 ± 5.2	(stat)
AKS inefficiency	1.2 ± 0.3	1.1 ± 0.4	
Reconstruction of $\pi^+\pi^-$	± 2.8	2.0 ± 2.8	
Reconstruction of $\pi^0\pi^0$	± 5.3	± 5.8	
Background to $\pi^+\pi^-$	14.2 ± 3.0	16.9 ± 3.0	
Background to $\pi^0\pi^0$	-5.6 ± 2.0	-5.9 ± 2.0	
Beam scattering	-8.8 ± 2.0	-9.6 ± 2.0	
Accidental tagging	6.9 ± 2.8	8.3 ± 3.4	(stat)
Tagging inefficiency	± 3.0	± 3.0	
Acceptance (statistical)	21.9 ± 3.5	26.7 ± 4.1	(stat)
(systematic)	± 4.0	± 4.0	
Accidental activity:			
intensity difference	± 1.1	± 3.0	
illumination difference	± 3.0	± 3.0	(stat)
K_S in time activity	± 1.0	± 1.0	
Total	$+35.0 \pm 6.5$	$+35.9 \pm 8.1$	(stat)
	± 9.0	± 9.6	

327 The residual acceptance correction is mostly due to beam geometry
 328 effects and is well evaluated by Monte Carlo simulation. Some system-
 329 atic uncertainties (indicated with “stat” in Table 2) are determined by
 330 the statistical significance of the control sample used.

331 The final result from 2001 data is $R = 0.99181 \pm 0.00147_{\text{stat}} \pm 0.00110_{\text{syst}}$,
 332 corresponding to $\text{Re}(\varepsilon'/\varepsilon) = (13.7 \pm 2.5_{\text{stat}} \pm 1.8_{\text{syst}}) \times 10^{-4}$. This result is in
 333 good agreement with the published value $\text{Re}(\varepsilon'/\varepsilon) = (15.3 \pm 2.6) \times 10^{-4}$,
 334 obtained from 1997–98-99 data at a different average beam intensity.
 335 Taking into account the correlated systematic uncertainty of $\pm 1.4 \times 10^{-4}$,
 336 the combined final result from the NA48 experiment is $\text{Re}(\varepsilon'/\varepsilon) = (14.7 \pm$
 337 $2.2) \times 10^{-4}$.

338 **References**

- 339 [1] J.H. Christenson et al., Phys. Rev. Lett. **13** (1964) 138.
340 [2] M. Kobayashi and K. Maskawa, Prog. Theor. Phys. **49** (1973) 652.
341 [3] M. Ciuchini, G. Martinelli, Nucl. Phys. **B** (Proc. Suppl.) **99B** (2001) 27;
342 E. Pallante et al., Nucl. Phys. **B** **617** (2001) 441;
343 A.J. Buras et al., Nucl. Phys. **B** **592** (2001) 55;
344 S. Bertolini et al., Phys. Rev. **D** **63** (2001) 056009;
345 Y.L. Wu, Phys. Rev. **D** **64** (2001) 0106001;
346 J. Donoghue, in: F. Costantini et al. (Eds), Proc. Int. Conf. on Kaon Physics
347 Frascati Physics Serie **26** (2001) p. 93;
348 T. Hambye et al., Nucl. Phys. **B** **564** (2000) 391;
349 J. Bijnens and J. Prades, JHEP **0006** (2000) 035;
350 T. Blum et al., hep-lat/0108013;
351 J.I. Noaki et al., hep-lat/0110075.
352 [4] G. Barr et al., Phys. Lett. **B** **317** (1993) 233.
353 [5] L.K. Gibbons et al., Phys. Rev. Lett. **70** (1993) 1203.
354 [6] A. Lai et al., Eur. Phys. J. **C** **22** (2001) 231–254.
355 [7] V. Fanti et al., Phys. Lett. **B** **465** (1999) 335–348.
356 [8] A. Glazov, KTeV Collaboration, in: F. Costantini et al. (Eds.), Proc. Int.
357 Conf. on Kaon Physics Frascati Physics Serie **26** (2001) p. 115.
358 [9] A. Alavi-Harati et al., Phys. Rev. Lett. **83** (1999) 22.
359 [10] C. Biino et al., CERN-SL-98-033(EA) and in: S. Myers, L. Liljeby and
360 C. Petit-Jean-Genaz (Eds), Proc. 6th EPAC, IOP, Bristol, 1999.
361 [11] P. Grafström et al., Nucl. Instr. Meth. **A** **344** (1994) 487;
362 H. Bergauer et al., Nucl. Instr. Meth. **A** **419** (1998) 623.
363 [12] R. Moore et al., Nucl. Instr. Meth. **B** **119** (1996) 149.
364 [13] D. Bèderède et al., Nucl. Instr. Meth. **A** **367** (1995) 88;
365 I. Augustin et al., Nucl. Instr. Meth. **A** **403** (1998) 472.
366 [14] G.D. Barr et al., Nucl. Instr. Meth. **A** **370** (1993) 413.
367 [15] G. Barr et al., Nucl. Instr. Meth. **A** **485** (2002) 676.
368 [16] S. Anvar et al., Nucl. Instr. Meth. **A** **419** (1998) 686.